



## Full length article

## Aminopyridines and 4-nitrophenol cocrystals for terahertz application

Mikhail N. Esaulkov<sup>a</sup>, Maria I. Fokina<sup>b</sup>, Natalia A. Zulina<sup>b</sup>, Tatiana V. Timofeeva<sup>b,c</sup>,  
Alexander P. Shkurinov<sup>a,d</sup>, Igor Yu. Denisjuk<sup>b,\*</sup>

<sup>a</sup> Institute on Laser and Information Technologies - Branch of the Federal Scientific Research Centre "Crystallography and Photonics" of Russian Academy of Sciences, Svyatoozerskaya 1, 140700, Shatura, Moscow Region, Russia

<sup>b</sup> School of Photonics, ITMO University, Kronverkskiy pr., 49, St. Petersburg, Russian Federation

<sup>c</sup> Department of Chemistry, New Mexico Highlands University, Las Vegas, NM 87701, USA

<sup>d</sup> Department of Physics and International Laser Center, Lomonosov Moscow State University, Leninskie Gory, Moscow, Russian Federation

## ARTICLE INFO

## Article history:

Received 30 December 2017

Received in revised form 26 June 2018

Accepted 14 July 2018

Available online 24 July 2018

## Keywords:

Nonlinear optical materials

Molecular crystals

Terahertz generation

Phase mismatch

Aminopyridine

4-nitrophenol

Co-crystal

## ABSTRACT

Co-crystals series of different mono- and diaminopyridines non-centrosymmetric complexes, namely 3,4-diaminopyridine-4-nitrophenol-4-nitrophenolate, 2,6-diaminopyridine-4-nitrophenol-4-nitrophenolate and 2-aminopyridine-4-nitrophenol-4-nitrophenolate were grown by slow solvent evaporation from solution with constant temperature technique. Terahertz absorption and refraction properties of the materials were measured, and the co-crystals were tested as generators of THz pulses under irradiation with 800 nm Ti:Sapphire femtosecond laser. Efficiency of the optical-to-THz conversion was compared to that of ZnTe crystal.

© 2018 Elsevier Ltd. All rights reserved.

## 1. Introduction

Within the last ten years, the field of terahertz science and technology has developed dramatically. Enormous amount of new and promising advances in the technology of terahertz generation and detection have been made. Most of successful studies in these scientific areas have been devoted to new materials and technology for terahertz generation and detection development [1]. Optical rectification in electro-optical crystals has been demonstrated as the best technique for generating subpicosecond pulses of electromagnetic radiation in the terahertz (THz) spectral range [2]. Many scientific groups have examined various nonlinear materials for THz emission under optical rectification. These materials include organic salts such as 4-*N,N*-dimethylamino-4-*N*-methylstilbazolium tosylate (DAST) [3], inorganic electro-optical materials like LiTaO<sub>3</sub>, LiNbO<sub>3</sub>, and semiconductors GaAs, GaSe, InAs, InP, GaP and others [4,5]. DAST co-crystal is one of the most efficient THz rectification material [6]. There are three important requirements for high efficiency of optical-to-terahertz conversion in non-linear optical crystals:

- High non-linear coefficients (susceptibility);
- Low intrinsic terahertz absorption of crystals;
- Phase matching conditions: difference between the group velocity for optical radiation at the central wavelength of the laser and phase velocity for THz radiation should be minimal in a broad frequency range in THz spectral region.

Phase matching is the major factor determining the efficiency of THz pulse generation and the bandwidth of emitted radiation. These conditions also determine the coherence length at desired THz frequency which helps the researcher to choose the optimal thickness of the nonlinear crystal for optimal balance between the amplitude and spectral bandwidth of emission.

Several organic crystals are known for exceptionally efficient optical rectification of femtosecond laser pulses: DAST, DSTMS, OH1, HMQ-TMS [7,8]. The phase matching conditions for these crystals are met for wavelengths of the optical pulse in the near infrared range (usually higher than 1  $\mu\text{m}$ ). However, the efficient organic nonlinear crystals for the middle of the operation range of most Ti:Sapphire lasers (near 0.8  $\mu\text{m}$ ) are lacking.

Among organic crystals applicable for THz emitting via optical rectification DAST co-crystal is most useful, because of its high thermostability up to 250°C, large EO coefficient and a low dielectric constant ( $\epsilon = 5.2$ ), giving a rise to a high modulator figure of

\* Corresponding author at: School of Photonics, ITMO University, Kronverkskiy pr., 49, St. Petersburg 197101, Russian Federation.

E-mail address: [denisiuk@mail.ifmo.ru](mailto:denisiuk@mail.ifmo.ru) (I.Yu. Denisjuk).

merit [9]. According to experimental data presented in [10], DAST exhibits the second-order NLO susceptibility  $\chi^{(2)} = 202 \pm 22$  pm/V at  $\lambda = 1318$  nm and the electro-optical figure of merit  $n^3 r_{11} = (53 \pm 6)$  pm/V at  $\lambda = 1313$  nm. Insignificant phase mismatch or even equality between terahertz and infrared (1.06  $\mu$ m) waves propagation velocity is another advantage of DAST co-crystal. However, very high price for DAST crystals and demand for using the femtosecond lasers with wavelength longer than 1  $\mu$ m encourage researchers to look for other non-linear organic crystals which would possess high efficiency and good phase matching at 0.8  $\mu$ m. Besides, as it shown in [11], DAST exist in at least three forms: two crystalline anhydrate forms showing strong nonlinear optical properties and hydrate form which is crystallized in an orange triclinic phase without substantial nonlinear response. Therefore, the presence of water vapor in air can cause the change in DAST morphology leading to loss of nonlinear properties, which is sometimes observed experimentally.

In our work, we study the promising candidates for THz applications: three aminopyridines – 4-nitrophenol based co-crystals, which are not hygroscopic and have high laser damage threshold [12]. For high second order nonlinear susceptibility synthesis of crystalline materials requires to orient donor-acceptor chromophores in non-centrosymmetric manner [13]. To obtain non-centrosymmetric packing, heterocyclic molecules of different aminopyridines were co-crystallized with NLO chromophore 4-nitrophenol (4N). Aminopyridine complexes are well-known series of compounds [14,15] with good optical properties, thermal stability [16] and suitability for optoelectronic devices. 4-Nitrophenol is a classic dipolar NLO chromophore, and the possibility of proton transfer from the OH group of 4-nitrophenol to various organic bases results in increasing of its molecular hyperpolarizability [14,17]. First report on these co-crystals structures was presented by Prakash et al. [14]. Their nonlinear properties in the optical range were investigated in our previous work [18].

One of the co-crystals from this series of aminopyridines was examined in the work [19]. In this study co-crystal 2,6-diaminopyridinium-4-nitrophenolate-4-nitrophenol prepared by same technique was used. Terahertz emission, THz spectra, and refractive index of the co-crystals were measured. The authors claimed the THz emission amplitude comparable to that of ZnTe crystal which encourages for further inspection of co-crystals of this series. However, it was mentioned that shape of crystals was not convenient for such measurements. It influenced on high light dispersion and incorrect measurement of optical absorption spectra, as a sum of optical absorption and dispersion loss, and possible incorrect measurements of terahertz properties.

In present research, we continue our previous study of several molecular aminopyridine – 4-nitrophenol co-crystals complexes [18] by using them as generators of broadband THz radiation induced by the femtosecond optical pulses of Ti:Sapphire laser at 800 nm. The results of terahertz measurements of a series of co-crystals of non-centrosymmetric complexes with good crystalline shapes 3,4-diaminopyridine-4-nitrophenol-4-nitrophenolate (34DAP4N), 2,6-diaminopyridine-4-nitrophenol-4-nitrophenolate (26DAP4N) and 2-aminopyridine-4-nitrophenol-4-nitrophenolate (2AP4N) are presented and discussed.

## 2. Material and methods

### 2.1. Synthesis and crystal growth

Initial components for crystals: 3,4-diaminopyridine (Aldrich, 54-96-6), 2,6-diaminopyridine (Aldrich, 141-86-6), 2-aminopyridine (Aldrich, 504-29-0), 4-nitrophenol (Aldrich, 100-02-7) are presented in Fig. 1. All of them were commercially

available and used without further purification. Crystals were grown by slow solvent evaporation technique at fixed temperature (from 18 till 35 °C, different for each system). This technique is widely used by several groups of scientists [14–16,20,21]. We followed the synthetic procedure of co-crystals production with 4-nitrophenol that was published by Prakash et al. [14]. Ethanol was used as a solvent. For the preparation of the solutions for co-crystallization, the components were dissolved in ethanol and mixed in 2:1 (4-nitrophenol: aminopyridine) molar ratio.

The mixture of solutions was stirred at room temperature for 1 h using magnetic stirrer. Continuous stirring ensured that obtained mixture of solutions is homogeneous. High purification level of synthesized compound was achieved by successive recrystallization of obtained crystals in the same solvent. The solution was filtered by funnel with quartz cells of micron size. A glass vessel with synthesized clear solution was covered with porous filter paper and placed into the thermostat at 25 °C for slow evaporation of the ethanol. After 15–30 days, 50% of solutions were evaporated and the crystals were grown (Fig. 2). Three types of co-crystals of 4-nitrophenol with different aminopyridines were grown successfully with sizes up to centimeters in one dimension for 34DAP4N, 26DAP4N and 2AP4N. According to our previous experience these crystals are not forming polymorphs when crystallized from different solvent. Their molecular and crystal structures are characterized using X-ray diffraction and results are described in detail in our work [16]. Obtained co-crystals, like most organic crystals, are fragile and can be destroyed by mechanical polishing, so the production of single crystals is important.

SHG conversion efficiency of the obtained single crystalline samples was measured by comparative SHG technique presented in our previous work [18]. An estimation of the nonlinear optical coefficient magnitude ( $d$ ), at 1064 nm, considering the thickness of the samples and the disordering of the crystalline regions that fall into the laser beam, gives values near: 13 pm/V for 34DAP4N, 21 pm/V for 26DAP4N and 39 pm/V for 2AP4N, which allows to consider these crystals as materials with high nonlinear optical parameters. These values of nonlinear coefficients of the co-crystals are quite sufficient for terahertz generation via optical rectification method.

Transparency of the materials in visible, UV and infrared ranges was studied with Shimadzu UV-1800 spectrophotometer in the range 190–1100 nm to show absence of light dispersion by threshold of absorption value near to crystalline absorption edge – 480 nm and high transmittance in transparent area.

For studies of THz transmission properties of the co-crystals we used a terahertz time-domain spectrometer schematically shown in Fig. 3. This spectrometer allows one to study the terahertz absorption and refraction properties of the co-crystals and the spectra of THz radiation, generated in the samples irradiated by femtosecond optical pulses. In this spectrometer, the THz radiation is generated when a femtosecond pulse from a Ti:Sapphire laser (Spectra Physics Tsunami, 797 nm, pulse width 120 fs, 80 MHz repetition rate) irradiates 1 mm thick (1 1 0) ZnTe crystal [22]. THz radiation is collimated and focused into free space using a pair of parabolic mirrors. For spectroscopic measurements, the sample is placed in the THz beam waist. After passing the sample, THz radiation is again collimated and refocused into the detector crystal using two off-axis parabolic mirrors. For detection of THz radiation, we use a 2-mm thick (1 1 0) ZnTe crystal and traditional electro-optical method (Fig. 3). The signal from the balanced detector is sent to lock-in amplifier for increasing the signal-to noise ratio. The pump beam is modulated at frequency 1300 Hz with a chopper, and this frequency is used as reference for the lock-in amplifier.

To study the THz generation in these co-crystals, we replace the ZnTe generator crystal with the sample under study. The energy of the femtosecond pulse has been kept at the same value for

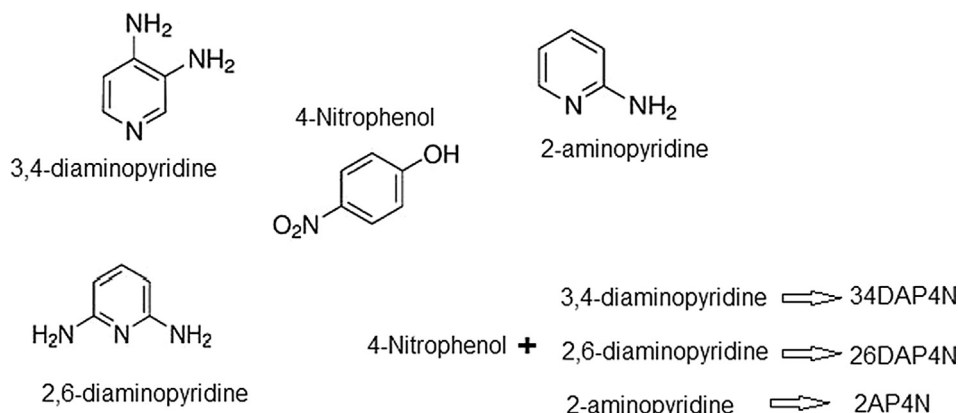


Fig. 1. Structural formulas of components.

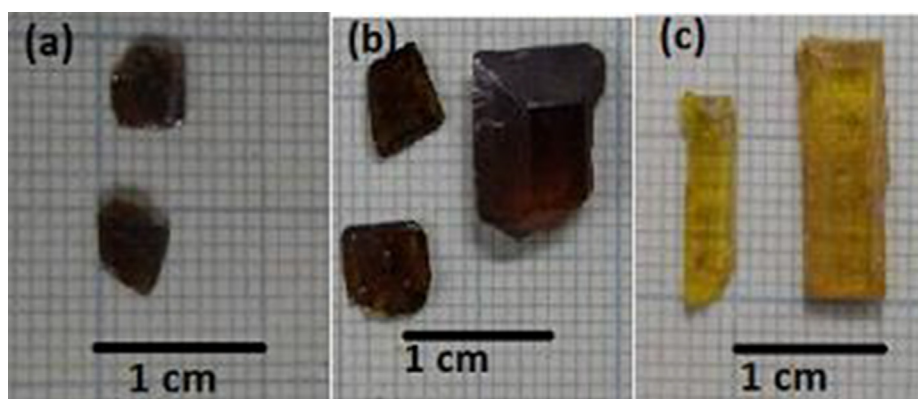


Fig. 2. Grown co-crystals of (a) 34DAP4N; (b) 26DAP4N and (c) 2AP4N.

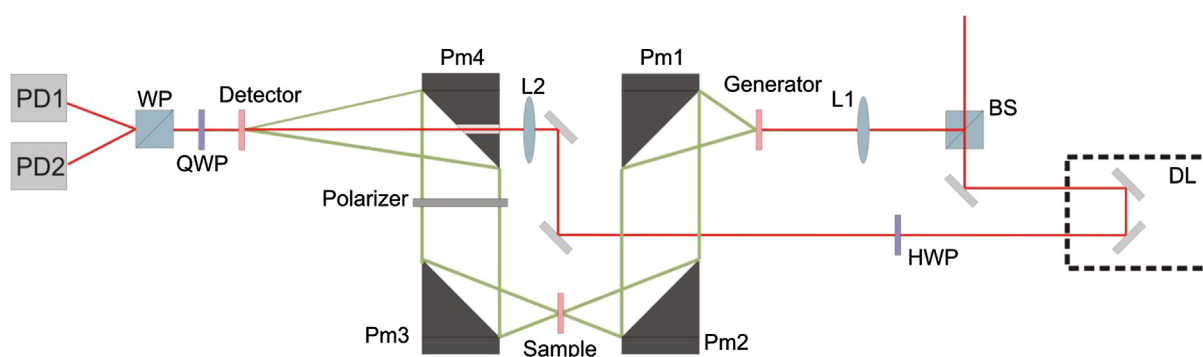


Fig. 3. Optical layout of THz-TDS spectrometer. L1, L2 – lenses, BS – beamsplitter (polarization cube), DL – motorized delay line, HWP – half-wave plate, Pm1-Pm4 – off-axis parabolic mirrors, QWP – quarter-wave plate, WP – Wollaston prism, PD1 and PD2 – balanced photodiodes.

comparison. The co-crystal was rotated by the azimuth angle and the waveforms were recorded for each rotation angle with 20° increment. Also, for qualitative analysis of polarization properties of generated radiation, we used a wire-grid THz polarizer in a collimated THz beam between 3rd and 4th parabolic mirror. The THz waveforms for vertically and horizontally oriented THz polarizer were measured.

The THz time-domain spectrometer allows one to estimate the group refractive index for optical radiation. To do this, we place the sample into a collimated optical beam before the THz generator and compare the time delay between the THz pulse with and without the sample in the optical beam path.

### 3. Results and discussion

#### 3.1. Absorption in UV and visible range

Obtained spectra of samples (Fig. 4) shows that crystals have wide and uniform transmittance having values from 50% to 80% up to 1100 nm from cutoff wavelength (420–474 nm), which we also observed in our previous work [18]. The homogeneity of the obtained crystals is confirmed by the optical transmittance spectra too - there is no monotonic increase in transmittance with an increase in the wavelength in the visible region, which indicates the absence of scattering by heterogeneities.

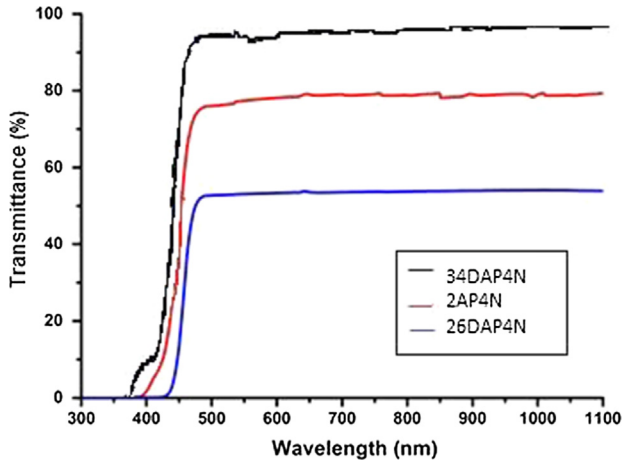


Fig. 4. Transmittance spectra of studied crystals.

### 3.2. Terahertz absorption and generation

All samples under study have shown strong birefringence in both optical and THz range. As a rule, the THz refractive index is higher than the group refractive index at 800 nm at any azimuth angle of the samples. For 26DAP4N the refractive indices for two orthogonal orientations are  $(2.1 \pm 0.2)$  and  $(1.7 \pm 0.2)$  for optical radiation at 800 nm and  $(2.4 \pm 0.2)$  and  $(1.9 \pm 0.2)$  for terahertz radiation respectively. For 2AP4N the refractive indices for two orthogonal orientations are  $(2.3 \pm 0.1)$  and  $(1.9 \pm 0.1)$  for optical radiation at 800 nm and  $(2.02 \pm 0.1)$  and  $(1.67 \pm 0.1)$  for terahertz radiation respectively. The 34DAP4N samples under study had very irregular shape, so it was hard to define the refraction indices for two orthogonal axes, but the values could be estimated as  $n_{\text{thz}} = 2.2$  and  $n_{\text{opt}} = 2$  for the orientation at which the highest THz generation was observed.

Since the refractive index for THz radiation is always higher than that for the optical radiation, the phase-matching conditions are not met in these co-crystals. That is why it is informative to use thin crystal samples for studying the THz generation efficiency. The coherence length for frequency 1 THz for the observed difference in refraction indices is approximately 0.6 mm in all three co-crystals. In our experiments, we used the following sample thicknesses: 0.9 mm for 26DAP4N, 0.6 mm for 34DAP4N, 0.41 mm for 2AP4N.

The samples have monotonically increasing absorption coefficient in 0.2–1.5 THz range which reaches 6–16  $\text{cm}^{-1}$  at 1 THz. The THz absorption spectra are shown in the Fig. 5, along with the refractive coefficient. We show here the absorption index

for the orientation of the co-crystal in which the highest THz generation efficiency was later observed, i.e. when the THz pulse polarization was parallel to the axis with low refractive index of the sample.

It is also worth mentioning that, despite the difference between the optical and THz refractive indices for the co-crystals, the refractive index for 2AP4N and 26DAP4N changes only slightly in 0.2–1.6 THz range. This means that for longer optical wavelengths, where the optical refractive index value is closer to that in the THz range, the phase matching conditions would be met in a rather broad spectral range which would result in generation of broadband THz pulses.

Generation of THz radiation in the co-crystals occurs predominantly at the same polarization as the polarization of femtosecond optical pulse. The amplitude of the THz radiation depends strongly on the azimuth rotation of the sample. As a rule, the efficiency of the optical-to-THz conversion is highest when axis of low refractive index of the sample coincides with the optical pulse polarization. In contrast, the efficiency of THz generation into orthogonal polarization is highest when the optical polarization direction coincides with the sample axis with the highest refractive index, but this efficiency is much lower than that in “all parallel” case. Fig. 6 shows the dependence of THz pulse amplitude on the azimuth angle of the sample for three types of co-crystals.

The spectra of THz radiation for all the co-crystals is broadband (see Fig. 7) and it spans from 0.2 to 2.5 THz (where the efficiency of THz detection in ZnTe drops substantially). This means that the use of such co-crystals for broadband THz spectroscopy can be prospective for other optical wavelengths (where the phase matching conditions are met and thick co-crystal samples can be used).

Finally, we compare the efficiencies of THz generation in the three co-crystals. For this, we use the formulas from [17]:

$$A_{\text{THz}} \propto FOM = \frac{d_{\text{eff}}^2 X}{n_{\text{opt}}^2 n_{\text{THz}}}$$

where  $FOM$  stands for so-called figure of merit of the THz emitter,  $d_{\text{eff}}$  is the nonlinear optical coefficient for optical rectification,  $n_{\text{opt}}$  and  $n_{\text{THz}}$  are the refractive indices in the optical and THz range,  $X$  is a multiplier which depends on the absorption of the emitter:  $X = L^2$  for materials with low absorption (lower than 5  $\text{cm}^{-1}$ ) and  $X = \frac{4}{\alpha^2}$  for materials with high absorption. Here,  $L$  is thickness of the emitter, and  $\alpha$  is its absorption coefficient.

The value  $d_{\text{eff}}$  for ZnTe is known (68 pm/V) [23] as well as its refraction indices and dimensions (length  $L = 0.3$  mm in our setup). To calculate the effective nonlinear coefficients for our co-crystals, we need to compare the measured peak THz field amplitudes for ZnTe and co-crystals (at their optimal orientations) and take into account the refraction indices and absorption coefficient (we take

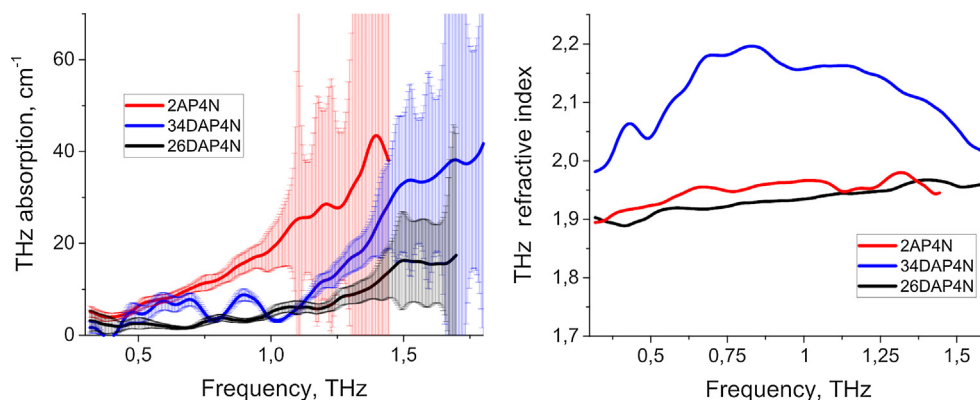
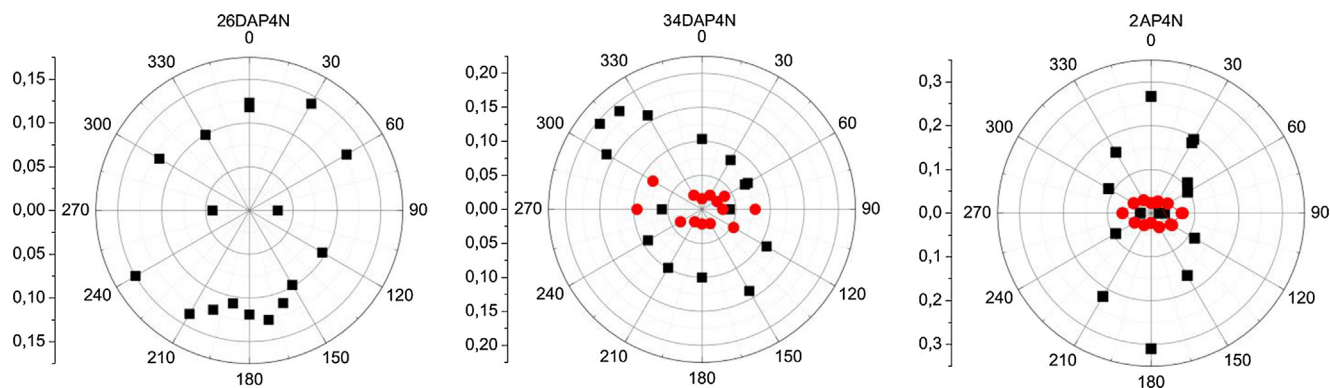
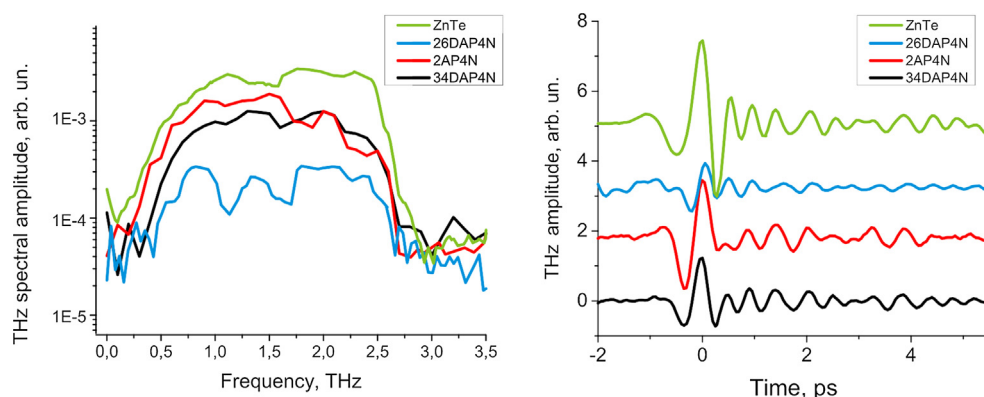


Fig. 5. Absorption coefficients for THz radiation for 26DAP4N, 34DAP4N and 2AP4N co-crystals (left) and refractive indices in the THz range for the same samples (right).





**Fig. 6.** Dependence of THz pulse amplitude on azimuth angle of the three samples. The optical pulse is polarized vertically. Azimuth angle 0° corresponds to position when crystal axis with low refractive index is vertical. Red dots show the amplitude of horizontally polarized THz radiation from the organic co-crystals, black squares – amplitude of vertically polarized THz radiation. (For interpretation of the references to colour in this figure legend, the reader is referred to the web version of this article.)



**Fig. 7.** Comparison between THz generation spectra in organic co-crystals and 0.3 mm thick ZnTe crystal. The right graph shows the waveforms of the THz pulse in each case.

**Table 1**  
The comparison of THz generation efficiencies of co-crystals and ZnTe crystal.

Material	Thickness, mm	THz amplitude, arb. un.	$d_{\text{eff}}$ , mV <sup>-1</sup>
ZnTe	0.3	0.234	$68 \cdot 10^{12}$
26DAP4N	0.9	0.083	$5 \pm 2 \cdot 10^{12}$
34DAP4N	0.6	0.123	$6 \pm 2 \cdot 10^{12}$
2AP4N	0.41	0.163	$10 \pm 3 \cdot 10^{12}$

it at 1 THz). The calculated values of  $d_{\text{eff}}$  are given in Table 1. The best THz waveforms for each material are shown in Fig. 7.

#### 4. Conclusion

We studied the emission and absorption properties in the THz range of three organic aminopyridines and 4-nitrophenol co-crystals. It was found that in the case of 2AP4N co-crystals amplitude of the emitted TH pulse can be comparable to that of the ZnTe crystal. The refractive index of the co-crystals remains at constant level in the 0.3–1.7 THz range for 2AP4N and 26DAP4N, which can ensure broadband THz generation in these materials. However, the phase matching conditions are not met for 800 nm radiation in all three co-crystals which requires using longer wavelengths for more efficient optical-to-THz conversion.

Easy method of their preparation and growth show possibility of future improvements by up-scaling crystal aperture size with relatively low cost. High laser damage threshold allows using high pump energies as well as applying shorter pump pulses. The lack of hygroscopicity and good atmospheric stability allows to use them without any additional atmospheric water protection. The condi-

tions for phase matching for broader optical range are subject of our future studies, as well as search for optimal conditions for growing thick uniform co-crystals for regular use in THz time-domain spectrometers. The presented results of terahertz emission by optical rectification in co-crystals can be applied for advanced THz technology including broadband THz time-resolved spectroscopy and high-resolution THz imaging.

#### Acknowledgments

Funding from Russian Foundation for Basic Research project № 18-52-16014, T. V. Timofeeva are grateful for support via NSF DMR-1523611 (PREM) and IIA-1301346 grants.

#### References

- [1] S.S. Dhillon, M.S. Vitiello, E.H. Linfield, A.G. Davies, M.C. Hoffmann, J. Booske, C. Paoloni, M. Gensch, P. Weightman, G.P. Williams, E. Castro-Camus, D.R.S. Cumming, F. Simoens, I. Escorcia-Carranza, J. Grant1, S. Lucyszyn, M. Kuwata-Gonokami, K. Konishi, M. Koch, C.A. Schmuttenmaer, T.L. Cocker, R. Huber1, A. G. Markelz, Z.D. Taylor, V.P. Wallace, J.A. Zeitler, J. Sibik, T.M. Korter, B. Ellison, S. Rea, P. Goldsmith, K.B. Cooper, R. Appleby, D. Pardo, P.G. Huggard, V. Kozar, H. Shams, M. Fice, C. Renaud, A. Seeds, A. Stöhr, M. Naftaly, N. Ridler, R. Clarke, J.E. Cunningham, M.B. Johnston, The 2017 terahertz science and technology roadmap, J. Phys. D: Appl. Phys. 50(49) (2017) 043001.
- [2] L. Xu, X.-C. Zhang, D.H. Auston, Terahertz beam generation by femtosecond optical pulses in electro-optic materials, Appl. Phys. Lett. 61 (1992) 1784–1792.
- [3] C.P. Yakymyshyn, K.R. Stewart, E.P. Boden, S.R. Marder, J.W. Perry, W.P. Schaefer, Second-order non-linear optical properties of 4n-methylstilbazolium tosylate salts, in: R.A. Hann, D. Bloor (Eds.), Organic Materials for Non-linear Optics II, Royal Society of Chemistry, London, 1991, pp. 108–114.
- [4] X. Mu, I.B. Zotova, Y.J. Ding, Power scaling on efficient generation of ultrafast terahertz pulses, IEEE J. Selected Topics Quantum Electron. 14 (2) (2008) 315–332.

- [5] A.G. Davies, E.H. Linfield, M.B. Johnston, The development of terahertz sources and their applications, *Phys. Med. Biol.* 47 (21) (2002) 3679.
- [6] A. Schneider, P. Günter, Spectrum of terahertz pulses from organic DAST crystals, *Ferroelectrics* 318 (1) (2005) 83–88.
- [7] C. Vicario, M. Jazbinsek, A.V. Ovchinnikov, O.V. Chefonov, S.I. Ashtkov, M.B. Agranat, C.P. Hauri, High efficiency THz generation in DSTMS, DAST and OH1 pumped by Cr: forsterite laser, *Opt. Exp.* 23 (4) (2015) 4573–4580.
- [8] J. Lu, H.Y. Hwang, X. Li, S.H. Lee, O.P. Kwon, K.A. Nelson, Tunable multi-cycle THz generation in organic crystal HMQ-TMS, *Opt. Exp.* 23 (17) (2015) 22723–22729.
- [9] F. Pan, G. Knopfle, Ch. Bosshard, S. Follonier, R. Spreiter, M. Wong, P. Gunter, Electro-optic properties of the organic salt 4-N, N-dimethylamino-4'-N'-methylstilbazolium tosylate, *J. Appl. Phys. Lett.* 69 (1996) 13–21.
- [10] B. Ruiz, M. Jazbinsek, P. Gunter, Crystal Growth of DAST, *J. Cryst. Growth Des.* 8 (2008) 4173–4184.
- [11] Y.W. Chen-Yang, T.J. Sheu, S.S. Lin, Y.K. Tu, Morphology and lightguide property investigation of a high quality DAST single crystal, *Curr. Appl. Phys.* 2 (5) (2002) 349–353.
- [12] I.I. M. Pavlovets, Sergiu Draguta, Maria I. Fokina, Tatiana V. Timofeeva, Igor Yu. Denisyuk, Organic noncentrosymmetric complexes of 4-nitrophenol for second harmonic generation, in: *Proceedings Volume 9532, Pacific Rim Laser Damage 2015: Optical Materials for High-Power Lasers*; 95320Y, 2015.
- [13] W. Robert, *Nonlinear Optics*, third ed., Academic Press, 2008.
- [14] M.J. Prakash, T.P. Radhakrishnan, SHG active salts of 4-nitrophenolate with H-bonded helical formations: structure-directing role of ortho-aminopyridines, *Cryst. Growth Des.* 5 (2) (2005) 721–725.
- [15] J. Zhao, P. Song, Y. Cui, X. Liu, S. Sun, S. Hou, F. Ma, Effects of hydrogen bond on 2-aminopyridine and its derivatives complexes in methanol solvent, *Spectrochim. Acta Part A* 131 (2014) 282–287.
- [16] K.M. Al-Ahmary, M.M. Habeeb, E.A. Al-Solmy, Spectroscopic studies of the hydrogen bonded charge transfer complex of 2-aminopyridine with  $\pi$ -acceptor chloranilic acid in different polar solvents, *J. Mol. Liquids* 162 (3) (2011) 129–134.
- [17] S. Draguta, M.S. Fonari, A.E. Masunov, J. Zazueta, S. Sullivan, M.Yu. Antipin, T.V. Timofeeva, New acentric materials constructed from aminopyridines and 4-nitrophenol, *Cryst. Eng. Comm.* 15 (2013) 4700–4710.
- [18] I.M. Pavlovets, S. Draguta, M.I. Fokina, T.V. Timofeeva, I.Y. Denisyuk, Synthesis, crystal growth, thermal and spectroscopic studies of acentric materials constructed from aminopyridines and 4-nitrophenol, *Opt. Comm.* 362 (2016) 64–68.
- [19] T. Chien-Ming, C. Li-Hsien, C. Yi-Cheng, P. Huang, M. Rajaboopathi, L. Chih-Wei, W. Kaung-Hsiung, V. Krishnakumar, T. Kobayashi, THz emission from organic cocrystalline salt: 2,6-diaminopyridinium-4-nitrophenolate-4-nitrophenol, *Opt. Exp.* 24 (5) (2016) 5039–5044.
- [20] M. Shkir, B. Riscob, G. Bhagavannarayana, Synthesis, growth, structural, spectroscopic, crystalline perfection, second harmonic generation (SHG) and thermal studies of 2-aminopyridinium picrate(2APP): a new nonlinear optical material, *Solid State Sci.* 14 (2012) 773–776.
- [21] P. Pandi, G. Peramaiyan, M.K. Kumar, R.M. Kumar, R. Jayavel, Synthesis, structural, optical and thermal studies of an organic nonlinear optical 4-aminopyridinium maleate single crystal, *Spectrochim. Acta Mol. Biomol. Spectrosc.* 88 (2012) 77–81.
- [22] M.M. Nazarov, S.A. Makarova, A.P. Shkurinov, O.G. Okhotnikov, The use of combination of nonlinear optical materials to control terahertz pulse generation and detection, *Appl. Phys. Lett.* 92 (2) (2008) 021114.
- [23] H. János, Ka-Lo Yeh, M.C. Hoffmann, B. Bartal, K.A. Nelson, Generation of high-power terahertz pulses by tilted-pulse-front excitation and their application possibilities, *JOSA B* 25 (7) (2008) B6–B19.